

Review: Ferromagnetism in Undoped ZrO₂ Thin Films

Shuai Ning and Zhengjun Zhang*

(Key Laboratory of Advanced Materials (MOE), School of Materials Science and Engineering, Tsinghua University, Beijing 100084, China)

Abstract: Diluted magnetic oxides have evolved into a popular branch of materials science during the last decade. In the first few years, people attributed the ferromagnetism to the magnetic dopants. However, the observation of ferromagnetism in undoped HfO₂ thin films made it more controversial and promoted extensive research on the ferromagnetism in various undoped oxides. Both of the experimental works and theoretical studies have shown that intrinsic defects in oxide nanomaterials play a crucial role in the origin of such an unexpected ferromagnetism, in spite of some contradicting views which kind of defects is predominant. In the past several years, we have conducted systematic and thorough research on the room temperature ferromagnetism in undoped ZrO₂ thin films, and clarify some physics behind it. We firstly prepared undoped ZrO₂ thin films by different ways, such as Pulsed electron beam deposition, magnetron sputtering, and electron beam evaporation, and successfully obtained ZrO₂ thin films with different crystalline structure, in particular a pure high-temperature stabilized one, by adjusting some preparation parameters during the deposition process or post-annealing treatment. A phase-dependent ferromagnetism was then confirmed to exist in such ZrO₂ thin films. Further, we conducted exhaustive defect analysis and characterization by X-ray photoelectron spectroscopy, photoluminescence spectra, and electron paramagnetic resonance, respectively, and found the oxygen vacancy, specifically the single ionized oxygen vacancy (V_o^+), has a remarkable influence on the enhancement of ferromagnetism. Herein, we will review the work in detail on the phase-dependent and oxygen vacancy-enhanced room temperature ferromagnetism in undoped ZrO₂ thin films.

Keywords: ZrO₂ thin film; ferromagnetism; phase-dependent; oxygen vacancy

CLC number: O484.1

Document code: A

Article ID: 1005-9113(2017)01-0001-10

1 Introduction

Ferromagnetic semiconductor or insulator is not new, and has fascinated considerable attention and interest since 1960 s, as it may play an important role in spintronics which has been developing into a most important branch of materials science due to the capability to generate and manipulate the electron spin, another freedom degree besides the electron charge. The hardest challenge here based on the manipulation of spins and charges at the same time is the material should possess both efficient spin-polarized carrier injection and transport^[1]. In the early times when ferromagnetic metals were employed as the contacts, the spin injection efficiency was always quite low as a consequence of the large mismatch of density of states (DOS) between the metal and semiconductor^[2-5]. That's why developing functional ferromagnetic semiconductor and insulator as spin-injection contacts seems to be quite imperative^[6]. However, earliest research showed that the Curie temperatures of most natural magnetic semiconductors were always very low which greatly limited their practical application^[7]. Making the semiconductor or insulator ferromagnetic above RT seems to be another challenge.

The first theoretical study on room temperature ferromagnetism (RTFM) in semiconductor is conducted by Dietl et al.^[8], and indicates the RTFM could be present in 5 at% Mn-doped GaN and ZnO, which triggers a new research hotspot, i. e. diluted magnetic semiconductor (DMS) or diluted magnetic oxide (DMO), and inspires many groups to participate in it, in particular after the subsequent experimental discovery of RTFM within Co-doped TiO₂ films^[9]. Since then, RTFM has been observed in various materials, especially in many kinds of wide-band-gap oxides doped by different elements, such as ZnO^[10-12], TiO₂^[13-15], SnO₂^[16-18], In₂O₃^[19-21], SrTiO₃^[22-24], etc., and is attributed to the interaction between the dopant moments and carrier spins of host^[25] via different theoretical models such as RKKY^[26-27], mean field theory^[28-29], or double exchange^[30-31], etc. However, someone is being suspicious whether the RTFM in doped DMS or DMO is intrinsic, since it may result from some metallic clusters and secondary phases which are easy to occur in those samples and might be detrimental to the practical application^[10].

The first observation of RTFM in HfO₂ thin films without any dopants and impurities by Coey et al.^[32-34] indicates that doping might not play any key roles in the

Received 2016-09-23.

Sponsored by the National Natural Science Foundation of China (Grant No. 50931002, 51072094 and 51372135), the Ministry of Education of the People's Republic of China (Grant No. 113007A) and the Tsinghua University Initiative Scientific Research Program.

* Corresponding author. E-mail: zjzhang@tsinghua.edu.cn.

RTFM of DMS or DMO, and makes the origin and mechanism of RTFM much more controversial, and challenges our understanding of such an unexpected d⁰ magnetism^[35] since neither Hf⁴⁺ nor O²⁻ were magnetic ions, and the d and f shells of Hf⁴⁺ ions were either empty or full. In the past decade, many groups have been involved in this field in order to get a better understanding of d⁰ magnetism. Actually, the RTFM has been observed in many kinds of undoped oxides, such as ZnO^[36], SnO₂^[37], TiO₂^[38], and Al₂O₃^[39], and is reported to be much sensitive to the growth conditions and considered to be strongly related to the defects within the materials. The influence on RTFM of various types of defects in DMO has been evaluated^[40–42], such as structure defects, surface defects, strain, and point defects like vacancies and interstitials, but the divergent views leave it still an open question, and encourage us to conduct systematic research on a certain oxide. Zirconia (ZrO₂) is one of the most important ceramic materials with widespread

application in structure materials, solid-state electrolytes, thermal barrier coatings, catalytic supports, oxygen gas sensors, and electro-optical materials^[43–44]. It is known to have three low-pressure crystalline structures, i.e. monoclinic (*m*), tetragonal (*t*) and cubic (*c*). The monoclinic phase (space group *P*2₁/*c*), stable at RT, transforms to the tetragonal phase (space group *P*4₂/nmc) around 1 400 K, and then to cubic phase (space group *Fm*3*m*) around 2 570 K^[45]. The c-ZrO₂ is predicted to be a promising candidate of DMO with Mn doping by theoretical calculation^[46]. Since then, many groups have taken part in the investigation of ferromagnetism in doped and undoped ZrO₂, but obtain a series of contradicting conclusions. Table 1 presents a list of recent results of ZrO₂-based DMO^[47–66], including the doping, crystalline structure, preparation method and magnetic order, which makes us much more interested in the magnetism in ZrO₂.

Table 1 Recent research work on the ZrO₂-based DMO

System	Phase	Preparation method	Magnetic order (RT)	Reference
Mn; ZrO ₂	m/t/c	PLD	Ferromagnetic	[47–48]
Mn; ZrO ₂	m/c	PLD	Ferromagnetic	[49]
Mn; ZrO ₂	c	Chemical method	Ferromagnetic	[50]
Mn; ZrO ₂	c	PLD	Ferromagnetic	[51]
Mn; ZrO ₂	t	Sol-gel method	Ferromagnetic	[52]
Mn; ZrO ₂	c	Coprecipitation	Nonmagnetic	[53]
Mn; ZrO ₂	c	Chemical method	Nonmagnetic	[54]
Mn; ZrO ₂	c	Sol-gel method	Nonmagnetic	[55]
Mn; ZrO ₂	t	Solid state method	Nonmagnetic	[56]
Fe; ZrO ₂	c	Microwave method	Ferromagnetic	[57]
Fe, Co; ZrO ₂	t	Sol-gel method	Ferromagnetic	[58]
Fe; ZrO ₂	t	Sol-gel method	Ferromagnetic	[59]
Fe; ZrO ₂	c	Coprecipitation	Nonmagnetic	[53]
Fe; ZrO ₂	m/t	Hydrothermal method	Nonmagnetic	[60]
Fe; ZrO ₂	t/c	Freeze-drying method	Paramagnetic	[61]
Cu; ZrO ₂	m/t	Incipient wetness impregnation	Paramagnetic	[62]
Ca; ZrO ₂	c	Chemical citratecombustion	Ferromagnetic	[63]
Mg; ZrO ₂	c	Chemical citratecombustion	Ferromagnetic	[63]
Undoped	m	PLD	Ferromagnetic	[47–48]
Undoped	m/t	Chemical citratecombustion	Ferromagnetic	[63]
Undoped	m	Purchased	Ferromagnetic	[64]
Undoped	m/t	PED	Ferromagnetic	[65]
Undoped	m/t	Sputtering	Ferromagnetic	[66]
Undoped	t	Sol-gel method	Ferromagnetic	[52]

In the following section, we will review our experimental work on the magnetism in ZrO_2 films without any dopants, which should be the first step to clarify whether ZrO_2 can exhibit ferromagnetism, and whether the ferromagnetism is intrinsic or not. In our work, based on the thorough analysis and characterization of intrinsic aspects, such as crystalline structure and oxygen defects, we are highly convinced that the intrinsic ferromagnetism in undoped ZrO_2 thin films is strongly dependent on the crystalline structure and can be enhanced by oxygen vacancy.

2 Experimental Section

To evaluate the effects of crystalline structure on the magnetism in ZrO_2 films, the high temperature phase of zirconia, i. e. $t\text{-ZrO}_2$ or $c\text{-ZrO}_2$, should be stabilized at RT firstly with non-doping methods, although doping is one of the most common ways to obtain the high temperature phase for traditional ZrO_2 ceramics^[67–68]. Given that the t - or $c\text{-ZrO}_2$ may also be stabilized at RT by sufficient oxygen vacancy or confining the grain size to nanoscale in thin films or nanocrystals, different physical vapor deposition methods, such as pulsed electron beam deposition (PED), magnetron sputtering, and electron beam evaporation, have been utilized to prepare undoped ZrO_2 films. By adjusting the preparation parameters during the deposition process and post-annealing treatment, the manipulation of crystalline structure of ZrO_2 films has been achieved successfully.

PED is first used to prepare ZrO_2 films on $\langle 100 \rangle$ Si substrate^[65]. It is observed that the ZrO_2 films with a thickness of ~ 100 nm exhibit a mixture of m and t phase, of which the ratio is dependent on the oxygen partial pressure during deposition (as shown in Fig.1). Specifically, for the ZrO_2 film deposited at an oxygen partial pressure of 9 mTorr, $m\text{-ZrO}_2$ is predominant, while for that deposited at higher oxygen partial pressure, the content of the $m\text{-ZrO}_2$ drastically decreases. We have also evaluated the influences on the ZrO_2 crystalline structure of others deposition parameters, such as substrate temperature and electron beam energy, but we still fail to obtain pure m - or $t\text{-ZrO}_2$ films, despite a significant manipulation of the two-phase ratio.

DC reactive magnetron sputtering is also utilized to prepare ZrO_2 films on $\langle 100 \rangle$ Si substrate^[66]. The crystalline structure of the obtained ZrO_2 films strongly depends on the flow rate ratio between oxygen and argon during the sputtering process. In all cases, the thickness of ZrO_2 films was controlled at ~ 200 nm. From Fig.2, when deposited at an O_2/Ar ratio of 1/19, the crystalline structure seems to be close to hexagonal

zirconium, indicating the oxygen partial pressure is not high enough to oxidize the metal Zr completely. The oxidation of zirconium is improved dramatically with the increase of the O_2/Ar ratio. When deposited at an O_2/Ar ratio of 2/18, the ZrO_2 films exhibit a nearly pure t phase, further confirmed by the good matching between the high-resolution transmission electron microscope (HRTEM) image and the schematic of the crystalline structure shown in Fig.3(a). When the ratio comes to 2.5/17.5, the $m\text{-ZrO}_2$ starts to appear, and then develops significantly with that increasing to 3/17. When that reaches 4/16, the ZrO_2 film seems to consist of only pure m phase, which can be also further confirmed by HRTEM image in Fig.3(b). The above results indicate the crystalline structure of ZrO_2 films may successfully be manipulated by adjusting the O_2/Ar ratio during preparation process, and that both of pure m - and $t\text{-ZrO}_2$ films can be stabilized at RT.

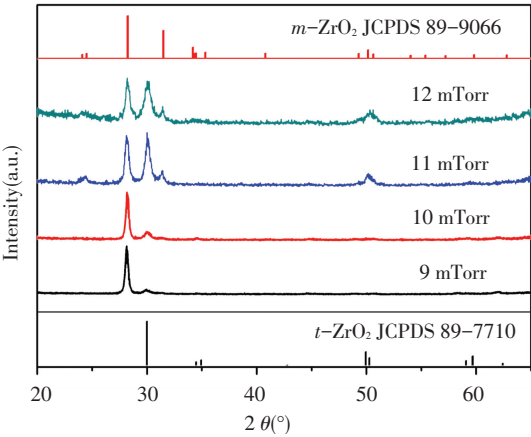


Fig.1 XRD results of ZrO_2 films prepared at different O_2 partial pressure by PED^[65]

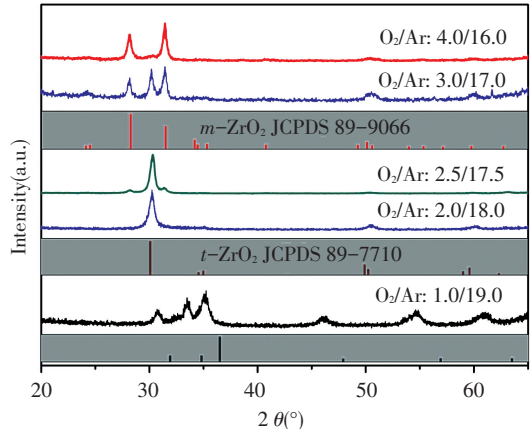


Fig.2 XRD results of ZrO_2 films prepared at different O_2/Ar ratio by sputtering^[66]

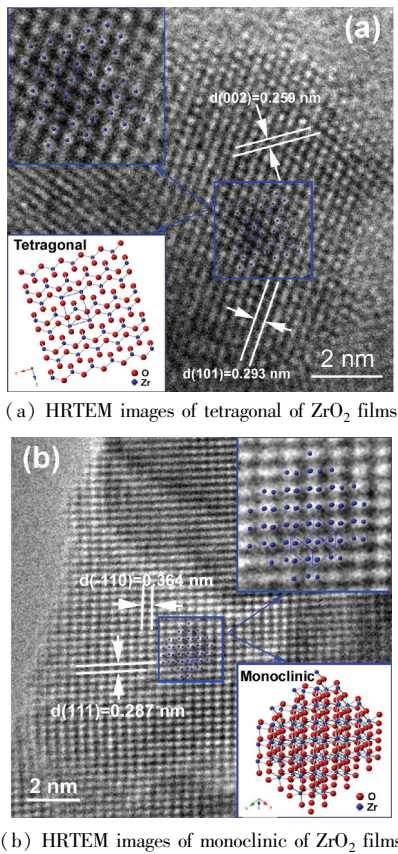


Fig.3 HRTEM images of tetragonal and monoclinic of ZrO₂ films, in which the inset shows the schematic of the corresponding crystalline structure^[69]

Electron beam evaporation is also used to prepare ZrO₂ films on $\langle 100 \rangle$ Si substrate. The as-grown 100 nm-thick films exhibit amorphous. In order to investigate the crystallization and phase transformation process of the amorphous ZrO₂ films, we conduct the in-situ optical reflectivity measurements based on the dependence of reflected optical power on the crystalline structure. Fig. 4 shows the in-situ reflected optical power versus the temperature, where the extreme point of the derivative of reflected power, specifically $\sim 320^\circ\text{C}$ can be regarded as a crystallization or phase transformation point. Then, the as-grown films are annealed at 320°C under air for 10 s, 10 min and 30 min respectively. XRD results demonstrate all the three annealed samples exhibit *t* phase, the high temperature one, unexpectedly. To assess the crystallization and phase transformation further, the as-grown films are annealed at 300°C , 500°C , 700°C , 900°C , and 1050°C for 10 s under air, respectively, by using rapid thermal annealing (RTA) system. The XRD results shown in Fig.5 indicate that the as-grown films still remain amorphous after annealing at 300°C , and crystallize fast and substantially into *t*-ZrO₂ after annealing at 320°C . With the increase of annealing temperature, a mixture of more *m*-ZrO₂ and less *t*-ZrO₂

is obtained. After annealed at 1050°C , it exhibits nearly pure *m*-ZrO₂ ultimately. The above results not only pave a simple and effective way to manipulate the ZrO₂ film crystalline structure, but also reveal some interesting underlying physics of the crystallization and phase transformation of amorphous ZrO₂ films, which deserve much more attention in the future.

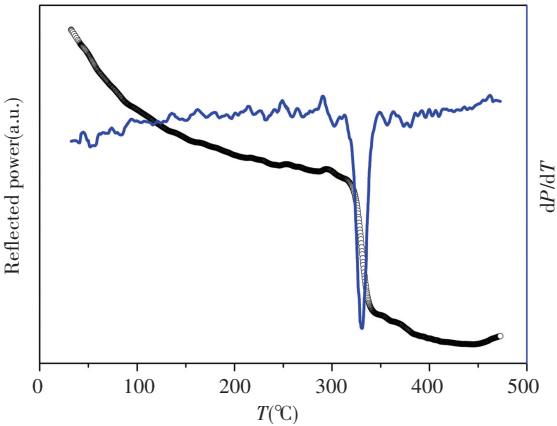


Fig. 4 The reflected optical power versus temperature of amorphous ZrO₂ films prepared by e-beam evaporation

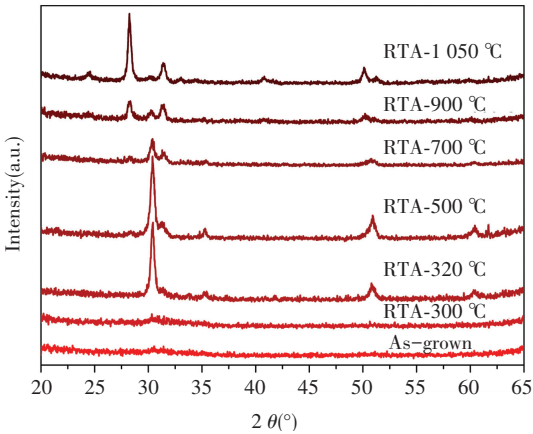


Fig.5 XRD results of ZrO₂ films annealed at different temperature in air by RTA

3 Results and Discussions

3.1 Ferromagnetism in Undoped ZrO₂ Films

The RT in-plane magnetic properties of ZrO₂ films with different crystalline structure prepared with all the above three methods are characterized. Fig.6 shows the hysteresis loops of the ZrO₂ films deposited at different oxygen partial pressures by PED, indicating RTFM exists in all the samples, the ~ 100 Oe coercivity can be easily observed from the inset of Fig. 6, an enlargement of the hysteresis loop of sample deposited at 11 mTorr. Given the crystalline structure shown in Fig.1, the normalized saturated magnetization (M_s)

seems to be positively dependent on the content of the t phase. Specifically, it is the minimum, ~ 0.04 emu/g, in the ZrO_2 film deposited at 9 mTorr in which m phase is predominant, and increases to the maximum, ~ 0.69 emu/g, in that deposited at 12 mTorr, in which the content of t phase is the largest.

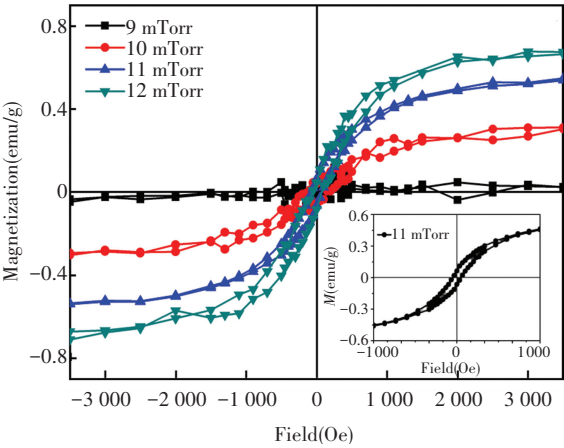


Fig.6 M - H curves of ZrO_2 films prepared at different O_2 partial pressure by PED^[65]

As for the samples prepared by sputtering, three representative ones are selected for the RT magnetic measurements, i. e. ZrO_2 film with a crystalline structure of m phase, t phase and the mixture. All the above samples exhibit intrinsic RTFM with a coercivity of ~ 50 Oe shown in Fig.7. The M_s of t - ZrO_2 film is the largest, 0.19 emu/g, and then gradually weakens with the decrease of the content of t phase, and almost destroys when the film only consists of m phase. It demonstrates that the RTFM in undoped ZrO_2 films prepared by sputtering also strongly depends on the crystalline structure.

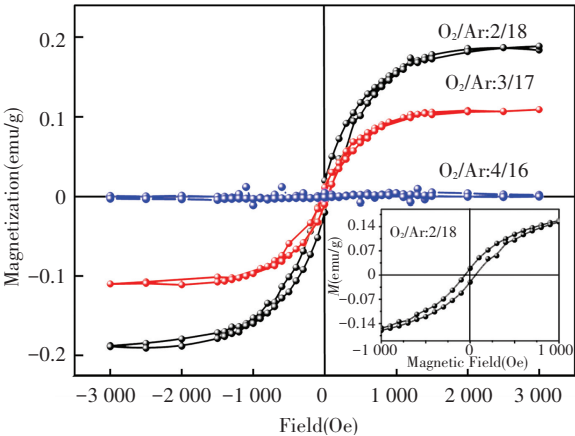


Fig.7 M - H curves of ZrO_2 films prepared at different O_2/Ar ratio by sputtering^[66]

The RT magnetic properties of ZrO_2 films annealed at different temperature by RTA, which are prepared by e-beam evaporation originally, has been also characterized. From the results depicted in Fig.8, a similar phase-dependent magnetism can be seen easily, that the normalized M_s is the largest for the ZrO_2 film with pure t phase, which is annealed at 320°C , and decreases gradually with decrease of t phase content, as a result of the increase of annealing temperature, and reaches the minimum for the sample with nearly pure m phase, which is annealed at 1050°C .

Taking all the above magnetism results into consideration, we are much convinced that the RTFM can be present intrinsically within the undoped ZrO_2 films, and it is strongly dependent on the crystalline structure, specifically, t phase is much more active to the RTFM than the m one.

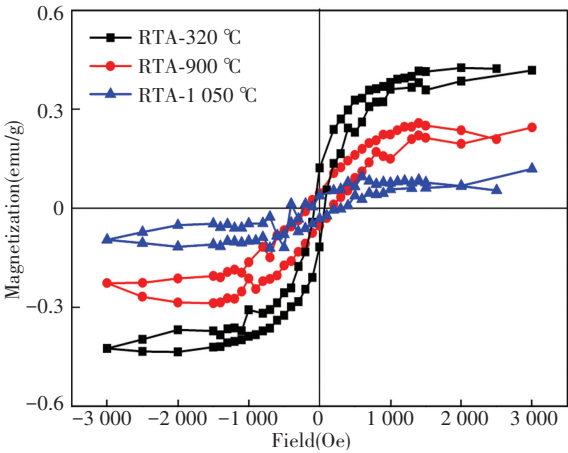


Fig.8 M - H curves of ZrO_2 films annealed at different temperature by RTA

3.2 Origin of Ferromagnetism in Undoped ZrO_2 Films

The non-equilibrium deposition process or the thermal annealing treatment can easily create various intrinsic defects that are predicted to be responsible for the unexpected d^0 magnetism in undoped DMO. A thorough defect analysis and characterization is of much necessity to evaluate the defect influence. Firstly, the high-resolution X-ray photoelectron spectroscopy (XPS) analysis on both of $\text{Zr } 3d$ and $\text{O } 1s$ core level for the samples prepared by sputtering is conducted. The results shown in Fig.9 consistently suggest that all the three samples are oxygen-deficient and the increase of O_2/Ar ratio significantly enhances the oxidation. In other words, the number of oxygen vacancy drastically decreases from the maximum in the sample with a pure t - ZrO_2 film, to the minimum in that with a pure m - ZrO_2 as the O_2/Ar ratio increases from 2/18 to 4/16.

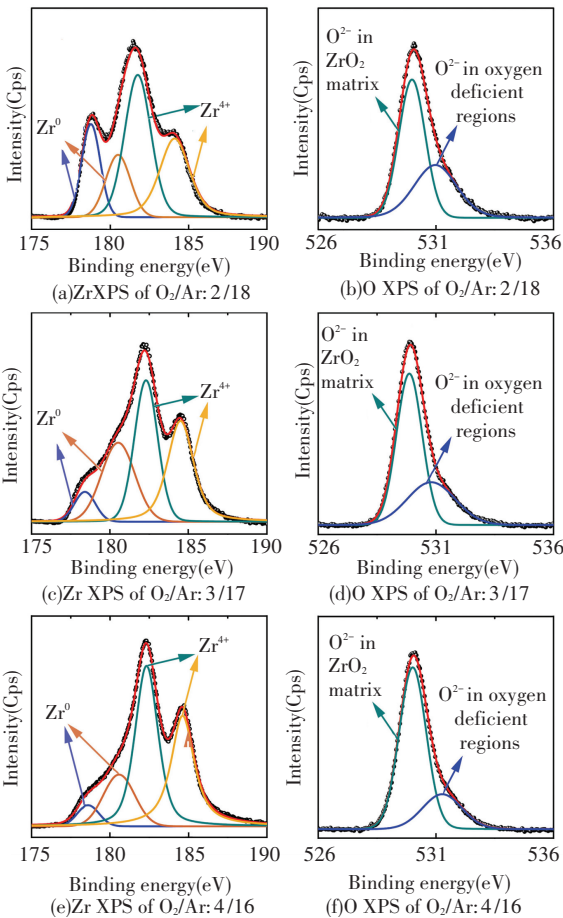


Fig.9 High resolution XPS of Zr 3d and O 1s core level of ZrO₂ films prepared at different O₂/Ar ratio by sputtering^[66]

Photoluminescence (PL) experiments are then conducted on the same samples with XPS measurements, and it reveals that the emission ascribed to oxygen vacancy drastically weakens (see Fig.10 (a)) in the ZrO₂ film deposited at a higher O₂/Ar ratio that consists of more *m* phase. The normalized *M_s* versus the intensity of PL emission originating from oxygen vacancy is plotted in Fig.10 (b), where a good positive linear relationship can be easily observed, demonstrating the oxygen vacancy can significantly enhance the RTFM in undoped ZrO₂ films. The electron paramagnetic resonance (EPR) is also conducted on the samples prepared by PED to investigate the defect state in more detail. The result in Fig.11(a) shows that each sample exhibits a peak at a *g* factor of ~2.001 originating from singly ionized oxygen vacancy (*V_o⁺*), a kind of typical paramagnetic defect^[70], and that the intensity, corresponding to the number of *V_o⁺*, is strongly dependent on the oxygen partial pressure. A positive correlation can be observed between the normalized *M_s* versus the EPR signal intensity (the height from peak to valley) from Fig.11

(b), furthering confirming the ferromagnetism in undoped ZrO₂ films is strongly related to the oxygen vacancy, in particular the *V_o⁺*.

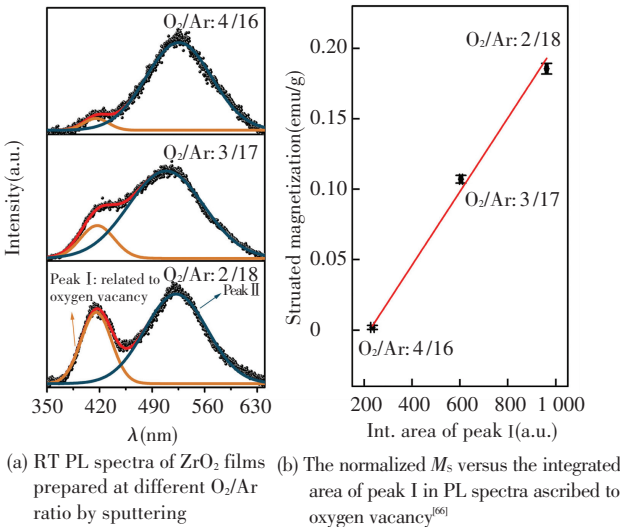


Fig.10 The relationship between magnetic property and PL results for the sputtering samples

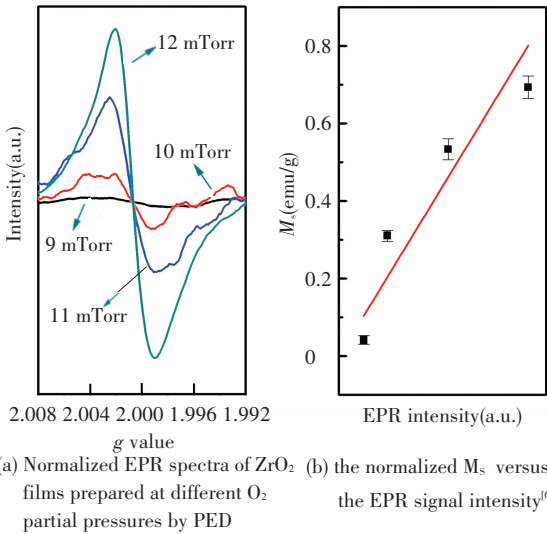


Fig.11 The relationship between magnetic property and EPR results for the PED samples

Taking both structure and oxygen defect analysis into account, it seems that the RTFM in undoped ZrO₂ films is not only dependent on the crystalline structure, but also on the number of oxygen vacancy. In order to clarify their respective contribution to the ferromagnetism, further validation experiments are then conducted. Firstly, the sample consisting of only *t*-ZrO₂ prepared by sputtering is annealed at 350 °C in air for 1 h. After annealing, it still remains pure *t* phase, but the RTFM almost disappears (see Fig.12 (b)). O 1s

core level XPS result after annealing shown in Fig.12 (a) suggests that oxygen deficiency is compensated to a large extent, indicating that the oxygen vacancy in *t*-ZrO₂ plays an important role in the origin or enhancement of RTFM in undoped ZrO₂ films. Likewise, the sample consisting of only *m*-ZrO₂ prepared by sputtering is also annealed at 350 °C in flowing Argon, an oxygen-deficient atmosphere, for 1 h. There are no changes in the crystalline structure, and no ferromagnetic signals appear in Fig.12(d), in spite of a significant reduction of ZrO₂ and increase of oxygen vacancy which can be seen from the O 1s core level XPS shown in Fig. 12 (c), indicating that the *m*-ZrO₂ could not exhibit ferromagnetic at RT even if it possesses a similar oxygen vacancy level with the *t*-ZrO₂. Then, it can be concluded that the intrinsic RTFM in undoped ZrO₂ films are indeed strongly dependent on the crystalline structure, and that *t*-ZrO₂ is much more active for the d⁰ magnetism that is driven or enhanced significantly by the oxygen vacancy.

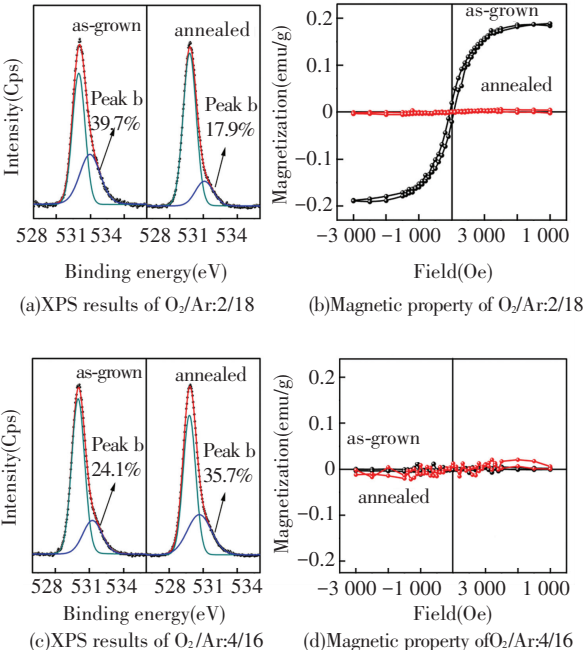


Fig.12 High resolution XPS of O 1s core level and *M-H* curves of the ZrO₂ films prepared at the O₂/Ar ratio of 2/18 and after annealed; high resolution XPS of O 1s core level and *M-H* curves of that prepared at the O₂/Ar ratio of 4/16 and after annealed^[66]

Then, one may also have a better understanding of the slight difference of the *M_s* values among three different kinds of preparation methods, shown in Figs.6–8, which may result from several aspects. For instance, the thickness was different in the three cases, and defects, including oxygen vacancy, are

much easier to be present in the region close to the interface. With the increase of film thickness, the crystallinity turns better and defects decrease drastically. That's why the samples prepared by sputtering with the larger thickness have lower *M_s* values. On the other hand, different preparation methods may result in a different number of oxygen vacancies within as-grown samples. As a consequence, the *M_s* may vary a little bit.

3.3 Mechanism of Oxygen Vacancy-Driven Ferromagnetism

Generally, two different theoretical models can be used to understand this oxygen vacancy-driven RTFM in DMOs, i. e. the percolation model of bound magneticpolaron (BMP)^[34] and charge transfer ferromagnetism (CTF)^[71]. For the BMP model, oxygen vacancy helps produce more BMPs and create a large overall volume occupied by BMPs. When the density of oxygen vacancy exceeds a certain threshold, it will lead to an overlap of BMPs and enhancing the ferromagnetic behavior^[72]. However, this model could not give a reasonable explanation on the absence of ferromagnetism in monoclinic samples despite a large number of oxygen vacancies after annealing in flowing Ar. For the CTF model, the idea is that a narrow, structured local density of states *N_s(E)* is associated with the defects, but the Fermi level will not normally locate as a peak in *N_s(E)*. A local charge reservoir, such as oxygen vacancies or cations with different charge states, provides a possibility for electron transfer to raise the Fermi level to a peak in the local density of states, leading to Stoner splitting of *N_s(E)*^[73] and triggering the ferromagnetism. In other words, the CTF depends not only on the vacancy levels, but also on the electronic band structure and density of states. It may give us a new thinking about the phase-dependent RTFM that we observed in undoped ZrO₂ thin films. As reported, the electronic band structure of tetragonal ZrO₂ is significantly different from that of monoclinic one^[74–76]. It is only in tetragonal ZrO₂ that the electron transferring from oxygen vacancies can raise the Fermi level to the peak in the local density of states and lead to spontaneous Stoner ferromagnetism, resulting in the different magnetic behavior between tetragonal and monoclinic samples with a similar oxygen vacancy level. Therefore, our results provide an experimental evidence for the CTF model to explain the magnetic ordering in undoped DMOs.

4 Conclusions

Undoped ZrO₂ film can be prepared by different physical vapor deposition, such as PED, sputtering

and e-beam evaporation. The crystalline structure can be manipulated successfully by adjusting the preparation parameters during the deposition process and post-annealing treatment. In particular, the high temperature phase, i.e. $t\text{-ZrO}_2$, can be stabilized at RT without any dopants, by sputtering at a proper oxygen partial pressure, or just annealing the amorphous samples prepared by e-beam evaporation at the critical crystallization temperature, which paves a simple way to investigate the phase-dependent properties of ZrO_2 films. Magnetic property characterization demonstrates that intrinsic ferromagnetism can be obtained in undoped ZrO_2 films, which seems to highly depend on the crystalline structure, as well as the oxygen defects in the films. Given the structure and defect analysis, the high temperature phase, i.e. $t\text{-ZrO}_2$, is found to be more active for the d^0 magnetism in undoped ZrO_2 films, and the ferromagnetism is strongly related with the oxygen vacancy.

In summary, in term of future applications, despite some progress of theoretical and experimental understanding, some details still remain unclear and appealing for much more attentions. Meanwhile, making use of DMO to design and fabricate prototype spintronic devices might also fascinate much more attention, which may become a new candidate for some new physical and multifunctional devices. We are pleased to see the progress of understanding of the d^0 magnetism and practical application of DMO in the near future.

References

- [1] Pearton S J, Heo W H, Ivill M, et al. Dilute magnetic semiconducting oxides. *Semiconductor Science and Technology*, 2004, 19(10): 59–74. DOI: 10.1088/0268-1242/19/10/R01.
- [2] Van Wees B J. Comment on “Observation of spin injection at a ferromagnet-semiconductor interface”. *Physical Review Letters*, 2000, 84(21): 5023. DOI: 10.1103/PhysRevLett.84.5023.
- [3] Schmidt G, Ferrand D, Molenkamp L W, et al. Fundamental obstacle for electrical spin injection from a ferromagnetic metal into a diffusive semiconductor. *Physical Review B*, 2000, 62(8): 4790–4793. DOI: 10.1103/PhysRevB.62.R4790.
- [4] Jonker B T, Kioseoglou G, Hanbicki A T, et al. Electrical spin-injection into silicon from a ferromagnetic metal/tunnel barrier contact. *Nature Physics*, 2007, 3(8): 542–546. DOI: 10.1038/nphys673.
- [5] Dash S P, Sharma S, Patel R S, et al. Electrical creation of spin polarization in silicon at room temperature. *Nature*, 2009, 462(7272): 491–494. DOI: 10.1038/nature08570.
- [6] Dietl T. A ten-year perspective on dilute magnetic semiconductors and oxides. *Nature Materials*, 2010, 9(12): 965–974. DOI: 10.1038/nmat2898.
- [7] Dietl T. Ferromagnetic semiconductors. *Semiconductor Science and Technology*, 2002, 17(4): 377. DOI: 10.1088/0268-1242/17/4/310.
- [8] Dietl T, Ohno H, Matsukura F, et al. Zener model description of ferromagnetism in zinc-blende magnetic semiconductors. *Science*, 2000, 287(5455): 1019–1022. DOI: 10.1126/science.287.5455.1019.
- [9] Matsumoto Y, Murakami M, Shono T, et al. Room-temperature ferromagnetism in transparent transition metal-doped titanium dioxide. *Science*, 2001, 291(5505): 854–856. DOI: 10.1126/science.1056186.
- [10] Kundaliya D C, Ogale S B, Lofland S E, et al. On the origin of high-temperature ferromagnetism in the low-temperature-processed Mn-Zn-O system. *Nature Materials*, 2004, 3(10): 709–714. DOI: 10.1038/nmat1221.
- [11] Herng T S, Qi D C, Berlijn T, et al. Room-temperature ferromagnetism of Cu-doped ZnO films probed by soft X-ray magnetic circular dichroism. *Physical Review Letters*, 2010, 105(20): 207201. DOI: 10.1103/PhysRevLett.105.207201.
- [12] Sharma P, Gupta A, Rao K V, et al. Ferromagnetism above room temperature in bulk and transparent thin films of Mn-doped ZnO. *Nature Materials*, 2003, 2(10): 673–677. DOI: 10.1038/nmat984.
- [13] Chambers S A, Thevuthasan S, Farrow R F, et al. Epitaxial growth and properties of ferromagnetic co-doped TiO_2 anatase. *Applied Physics Letters*, 2001, 79(21): 3467–3469. DOI: 10.1063/1.1420434.
- [14] Kim J Y, Park J H, Park B G, et al. Ferromagnetism Induced by Clustered Co in Co-Doped Anatase TiO_2 Thin Films. *Physical Review Letters*, 2003, 90(1): 017401. DOI: 10.1103/PhysRevLett.90.017401.
- [15] Griffin K A, Pakhomov A B, Wang C M, et al. Intrinsic ferromagnetism in insulating cobalt doped anatase TiO_2 . *Physical Review Letters*, 2005, 94(15): 157204. DOI: 10.1103/PhysRevLett.94.157204.
- [16] Ogale S B, Choudhary R J, Buban J P, et al. High temperature ferromagnetism with a giant magnetic moment in transparent co-doped $\text{SnO}_{2-\delta}$. *Physical Review Letters*, 2003, 91(7): 077205. DOI: 10.1103/PhysRevLett.91.077205.
- [17] Hays J, Punnoose A, Baldner R, et al. Relationship between the structural and magnetic properties of Co-doped SnO_2 nanoparticles. *Physical Review B*, 2005, 72(7): 075203. DOI: 10.1103/PhysRevB.72.075203.
- [18] Fitzgerald C B, Venkatesan M, Dorneles L S, et al. Magnetism in dilute magnetic oxide thin films based on SnO_2 . *Physical Review B*, 2006, 74(11): 115307. DOI: 10.1103/PhysRevB.74.115307.
- [19] Nguyen H H, Sakai J, Ngo T H, et al. Room temperature ferromagnetism in laser ablated Ni-doped In_2O_3 thin films. *Applied Physics Letters*, 2005, 87: 102505. DOI: 10.1063/1.2041822.
- [20] Peleckis G, Wang X, Dou S X. Room-temperature ferromagnetism in Mn and Fe codoped In_2O_3 . *Applied Physics Letters*, 2006, 88: 132507. DOI: 10.1063/1.2191093.
- [21] Panguluri R P, Kharel P, Sudakar C, et al. Ferromagnetism and spin-polarized charge carriers in In_2O_3 thin films. *Physical Review B*, 2009, 79(16): 165208. DOI: 10.1103/PhysRevB.79.165208.
- [22] Kim D H, Bi L, Jiang P, et al. Magnetoelastic effects in $\text{SrTi}_{1-x}\text{M}_x\text{O}_3$ ($\text{M} = \text{Fe}, \text{Co}, \text{or Cr}$) epitaxial thin films. *Physical Review B*, 2011, 84(1): 014416. DOI: 10.1103/PhysRevB.84.014416.

- 1103/PhysRevB.84.014416.
- [23] Posadas A B, Mitra C, Lin C, et al. Oxygen vacancy-mediated room-temperature ferromagnetism in insulating cobalt-substituted SrTiO₃ epitaxially integrated with silicon. *Physical Review B*, 2013, 87 (14): 144422. DOI: 10.1103/PhysRevB.87.144422.
- [24] Mitra C, Lin C, Posadas A B, et al. Role of oxygen vacancies in room-temperature ferromagnetism in cobalt-substituted SrTiO₃. *Physical Review B*, 2014, 90 (12): 125–130. DOI: 10.1103/PhysRevB.90.125130.
- [25] Ogale S B. Dilute doping, defects, and ferromagnetism in metal oxide systems. *Advanced Materials*, 2010, 22(29): 3125–3155. DOI: 10.1002/adma.200903891.
- [26] Priour D J, Sarma S D. Phase diagram of the disordered RKKY model in dilute magnetic semiconductors. *Physical Review Letters*, 2006, 97(12): 127201. DOI: 10.1103/PhysRevLett.97.127201.
- [27] Calderon M J, Sarma S D. Theory of carrier mediated ferromagnetism in dilute magnetic oxides. *Annals of Physics*, 2007, 322(11): 2618–2634. DOI: 10.1016/j.aop.2007.01.010.
- [28] Priour D J, Hwang E H, Sarma S D. Disordered RKKY lattice mean field theory for ferromagnetism in diluted magnetic semiconductors. *Physical Review Letters*, 2004, (11): 117201. DOI: 10.1103/PhysRevLett.92.117201.
- [29] Meilikhov E Z. Diluted magnetic semiconductors with correlated impurities: mean-field theory with RKKY interaction. *Physical Review B*, 2007, 75 (4): 045204. DOI: 10.1103/PhysRevB.75.045204.
- [30] Blinowski J, Kacman P. Double exchange in mixed-valency diluted magnetic semiconductors. *Acta Physica Polonica-Series A General Physics*, 1996, 90(4): 731–734.
- [31] Fleurov V, Kikoin K, Ivanov V A, et al. Mechanisms of double magnetic exchange in dilute magnetic semiconductors. *Journal of Magnetism and Magnetic Materials*, 2004, 272: 1967 – 1968. DOI: 10.1016/j.jmmm.2003.12.1067.
- [32] Venkatesan M, Fitzgerald C B, Coey J M. Thin films: unexpected magnetism in a dielectric oxide. *Nature*, 2004, 430(7000): 630. DOI: 10.1038/430630a.
- [33] Coey J M, Venkatesan M U, Stamenov P, et al. Magnetism in hafnium dioxide. *Physical Review B*, 2005, 72(2): 024450. DOI: 10.1103/PhysRevB.72.024450.
- [34] Coey J M, Venkatesan M, Fitzgerald C B. Donor impurity band exchange in dilute ferromagnetic oxides. *Nature Materials*, 2005, 4 (2): 173 – 179. DOI: 10.1038/nmat1310.
- [35] Coey J M. d⁰ ferromagnetism. *Solid State Sciences*, 2005, 7(6): 660 – 667. DOI: 10.1016/j.solidstatesciences.2004.11.012.
- [36] Xu Q, Schmidt H, Zhou S, et al. Room temperature ferromagnetism in ZnO films due to defects. *Applied Physics Letters*, 2008, 92(8): 082508. DOI: 10.1063/1.2885730.
- [37] Chen Z Y, Chen Z Q, Pan R K, et al. Vacancy-induced ferromagnetism in SnO₂ nanocrystals: a positron annihilation study. *Chinese Physics Letters*, 2013, 30 (2): 027804. DOI: 10.1088/0256-307X/30/2/027804.
- [38] Hong N H, Sakai J, Poirot N, et al. Room-temperature ferromagnetism observed in undoped semiconducting and insulating oxide thin films. *Physical Review B*, 2006, 73 (13): 132404. DOI: 10.1103/PhysRevB.73.132404.
- [39] Yang G, Gao D, Zhang J, et al. Evidence of vacancy-induced room temperature ferromagnetism in amorphous and crystalline Al₂ O₃ nanoparticles. *The Journal of Physical Chemistry C*, 2011, 115(34): 16814. DOI: 10.1021/jp2039338.
- [40] Pemmaraju C D, Sanvito S. Ferromagnetism driven by intrinsic point defects in HfO₂. *Physical Review Letters*, 2005, 94(21): 217205. DOI: 10.1103/PhysRevLett.94.217205.
- [41] Dev P, Xue Y, Zhang P. Defect-induced intrinsic magnetism in wide-gap III nitrides. *Physical Review Letters*, 2008, 100 (11): 117204. DOI: 10.1103/PhysRevLett.100.117204.
- [42] Peng H, Li J, Li S S, et al. Possible origin of ferromagnetism in undoped anatase TiO₂. *Physical Review B*, 2009, 79(9): 092411. DOI: 10.1103/PhysRevB.79.092411.
- [43] Steiner S A, Baumann T F, Bayer B C, et al. Nanoscale zirconia as a nonmetallic catalyst for graphitization of carbon and growth of single-and multiwall carbon nanotubes. *Journal of the American Chemical Society*, 2009, 131 (34): 12144 – 12154. DOI: 10.1021/ja902913r.
- [44] Cheema T A, Garnweitner G. Phase-controlled synthesis of ZrO₂ nanoparticles for highly transparent dielectric thin films. *CrystEngComm*, 2014, 16(16): 3366–3375. DOI: 10.1039/C3CE42392A.
- [45] Zhao X, Vanderbilt D. Phonons and lattice dielectric properties of zirconia. *Physical Review B*, 2002, 65(7): 075105. DOI: 10.1103/PhysRevB.65.075105.
- [46] Ostanin S, Ernst A, Sandratskii L M, et al. Mn-stabilized zirconia: From imitation diamonds to a new potential high-T_c ferromagnetic spintronics material. *Physical Review Letters*, 2007, 98 (1): 016101. DOI: 10.1103/PhysRevLett.98.016101.
- [47] Zippel J, Lorenz M, Setzer A, et al. Defect-induced ferromagnetism in undoped and Mn-doped zirconia thin films. *Physical Review B*, 2010, 82(12): 125209. DOI: 10.1103/PhysRevB.82.125209.
- [48] Zippel J, Lorenz M, Setzer A, et al. Defect-induced magnetism in homoepitaxial manganese-stabilized zirconia thin films. *Journal of Physics D: Applied Physics*, 2013, 46(27): 275002. DOI: 10.1088/0022-3727/46/27/275002.
- [49] Hong N H, Park C K, Raghavender A T, et al. Room temperature ferromagnetism in monoclinic Mn-doped ZrO₂ thin films. *Journal of Applied Physics*, 2012, 111(7): 07C302. DOI: 10.1063/1.3670577.
- [50] Clavel G, Willinger M G, Zitoun D, et al. Manganese-doped zirconia nanocrystals. *European Journal of Inorganic Chemistry*, 2008, 2008(6): 863–868. DOI: 10.1002/ejic.200700977.
- [51] Hong N H, Park C K, Raghavender A T, et al. High temperature ferromagnetism in cubic Mn-doped ZrO₂ thin films. *Journal of Magnetism and Magnetic Materials*, 2012, 324(19): 3013–3016. DOI: 10.1016/j.jmmm.2012.04.047.
- [52] Kumar S, Ojha A K. Room temperature ferromagnetism in undoped and Mn doped *t*-ZrO₂ nanostructures originated due to oxygen vacancy and effect of Mn doping on its optical properties. *Materials Chemistry and Physics*, 2016, 169: 13–20. DOI: 10.1016/j.matchemphys.2015.11.018.

- [53] Yu J, Duan L B, Wang Y C, et al. Absence of ferromagnetism in Mn- and Fe-stabilized zirconia nanoparticles. *Physica B: Condensed Matter*, 2008, 403 (23): 4264–4268. DOI: 10.1016/j.physb.2008.09.015.
- [54] Dimri M C, Kooskora H, Pahapill J, et al. Search for ferromagnetism in manganese-stabilized zirconia. *Physica Status Solidi (a)*, 2011, 208 (1): 172–179. DOI: 10.1002/pssa.201026304.
- [55] Pucci A, Clavel G, Willinger M G, et al. Transition metal-doped ZrO_2 and HfO_2 nanocrystals. *The Journal of Physical Chemistry C*, 2009, 113 (28): 12048–12058. DOI: 10.1021/jp9029375.
- [56] Srivastava S K, Lejay P, Barbara B, et al. Absence of ferromagnetism in Mn-doped tetragonal zirconia. *Journal of Applied Physics*, 2011, 110 (4): 043929. DOI: 0.1063/1.3626788.
- [57] Sahoo T R, Manoharan S S, Kurian S, et al. Mössbauer spectroscopic study of iron-doped zirconia synthesized by microwave route. In ICAME 2007. Berlin: Springer Berlin Heidelberg, 2008. 1277–1283.
- [58] Okabayashi J, Kono S, Yamada Y, et al. Fabrication and magnetic properties of Fe and Co co-doped ZrO_2 . *AIP Advances*, 2011, 1 (4): 042138. DOI: 10.1063/1.3662044.
- [59] Bashir M, Riaz S, Farooq M, et al. Structural and Magnetic Properties of Fe_3O_4 Doped Zirconia. *Materials Today: Proceedings*, 2015, 2 (10): 5611–5618. DOI: 10.1016/j.matpr.2015.11.098.
- [60] Kuryliszyn-Kudelska I, Arciszewska M, Małolepszy A, et al. Influence of Fe doping on magnetic properties of ZrO_2 nanocrystals. *Journal of Alloys and Compounds*, 2015, 632: 609–616. DOI: 10.1016/j.jallcom.2015.01.257.
- [61] De Souza A O, Ivashita F F, Biondo V, et al. Structural and magnetic properties of iron doped ZrO_2 . *Journal of Alloys and Compounds*, 2016, 680: 701–710. DOI: 10.1016/j.jallcom.2016.04.170.
- [62] Dutta P, Seehra M S, Zhang Y, et al. Nature of magnetism in copper-doped oxides: ZrO_2 , TiO_2 , MgO , SiO_2 , Al_2O_3 , and ZnO . *Journal of Applied Physics*, 2008, 103 (7): 07D104. DOI: 10.1063/1.2830555.
- [63] Dimri M C, Khanduri H, Kooskora H, et al. Room-temperature ferromagnetism in Ca and Mg stabilized cubic zirconia bulk samples and thin films prepared by pulsed laser deposition. *Journal of Physics D: Applied Physics*, 2012, 45 (47): 475003. DOI: 10.1088/0022-3727/45/47/475003.
- [64] Wang D D, Qi N, Jiang M, et al. Defects versus grain size effects on the ferromagnetism of ZrO_2 nanocrystals clarified by positron annihilation. *Applied Physics Letters*, 2013, 102 (4): 042407. DOI: 10.1063/1.4790156.
- [65] Ning S, Zhan P, Xie Q, et al. Room-temperature ferromagnetism in un-doped ZrO_2 thin films. *Journal of Physics D: Applied Physics*, 2013, 46 (44): 445004. DOI: 10.1088/0022-3727/46/44/445004.
- [66] Ning S, Zhang Z J. Phase-dependent and defect-driven d^0 ferromagnetism in undoped ZrO_2 thin films. *RSC Advances*, 2015, 5 (5): 3636–3641. DOI: 10.1039/C4RA11924J.
- [67] Pazhani R, Kumar H P, Varghese A, et al. Synthesis, vacuum sintering and dielectric characterization of zirconia ($t\text{-ZrO}_2$) nanopowder. *Journal of Alloys and Compounds*, 2011, 509 (24): 6819–6823. DOI: 10.1016/j.jallcom.2011.03.089.
- [68] Sayan S, Nguyen N V, Ehrstein J, et al. Structural, electronic, and dielectric properties of ultrathin zirconia films on silicon. *Applied Physics Letters*, 2005, 86 (15): 152902. DOI: 10.1063/1.1864235.
- [69] Ning S, Zhan P, Xie Q, et al. Defects-driven ferromagnetism in undoped dilute magnetic oxides: a review. *Journal of Materials Science & Technology*, 2015, 31 (10): 969–978. DOI: 10.1016/j.jmst.2015.08.011.
- [70] Liu H, Zeng F, Lin Y, et al. Correlation of oxygen vacancy variations to band gap changes in epitaxial ZnO thin films. *Applied Physics Letters*, 2013, 102 (18): 181908. DOI: 10.1063/1.4804613.
- [71] Coey J M, Wongsaprom K, Alaria J, et al. Charge-transfer ferromagnetism in oxide nanoparticles. *Journal of Physics D: Applied Physics*, 2008, 41 (13): 134012. DOI: 10.1088/0022-3727/41/13/134012.
- [72] Santara B, Giri P K, Imakita K, et al. Evidence of oxygen vacancy induced room temperature ferromagnetism in solvothermally synthesized undoped TiO_2 nanoribbons. *Nanoscale*, 2013, 5 (12): 5476–5488. DOI: 10.1039/C3NR00799E.
- [73] Song C, Pan F. *Transition Metal-Doped Magnetic Oxides. Oxide Semiconductors*. Elsevier, 2013. 227–259.
- [74] Kralik B, Chang E K, Louie S G. Structural properties and quasiparticle band structure of zirconia. *Physical Review B*, 1998, 57 (12): 7027. DOI: 10.1103/PhysRevB.57.7027.
- [75] French R H, Glass S J, Ohuchi F S, et al. Experimental and theoretical determination of the electronic structure and optical properties of three phases of ZrO_2 . *Physical Review B*, 1994, 49 (8): 5133. DOI: 10.1103/PhysRevB.49.5133.
- [76] Nawale A B, Kanhe N S, Bhoraskar S V, et al. Influence of crystalline phase and defects in the ZrO_2 nanoparticles synthesized by thermal plasma route on its photocatalytic properties. *Materials Research Bulletin*, 2012, 47 (11): 3432–3439. DOI: 10.1016/j.materresbull.2012.07.010.